Supporting information for

Constructing high-performance zinc metal anodes based on amino-functionalized highly three-dimensional porous structure interface layer

Shuo Li, Yingxiao Du, Xinyan Zhu, Ningning Zhao,* Lei Dai,* Bin Li, Zekun Zhang, Wei Meng, Jing Zhu, Ling Wang, Zhangxing He*

School of Chemical Engineering, North China University of Science and Technology, Tangshan 063210, China.

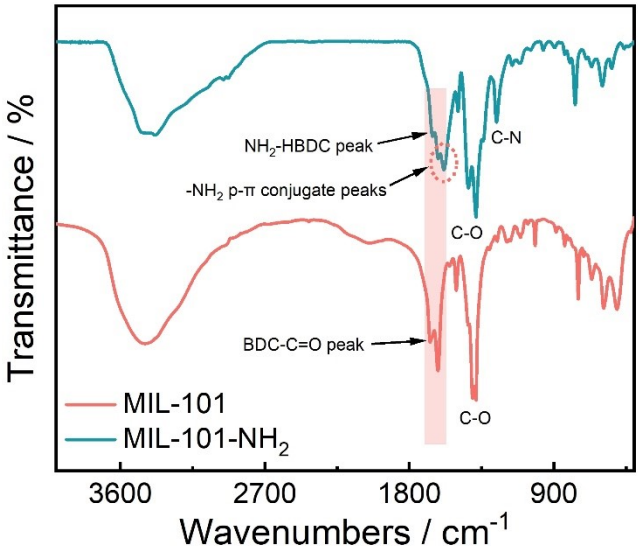

Fig. S1 FT-IR spectra of MIL-101-NH_2 and MIL-101.

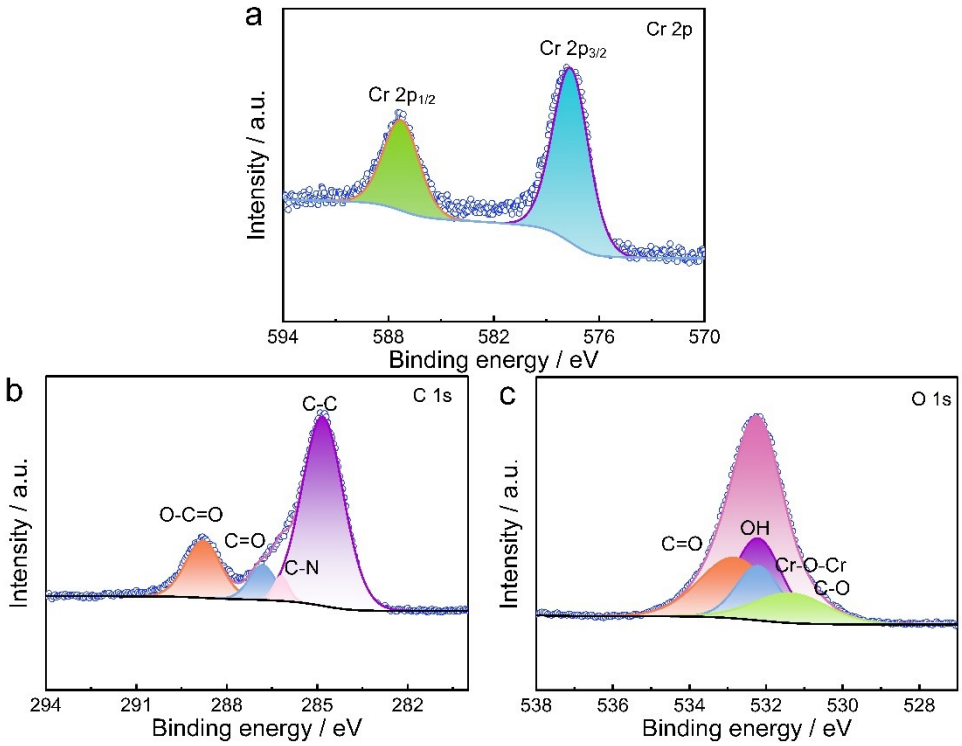

Fig. S2 XPS high resolution spectra of (a) Cr 2p, (b) C1s and (c) O 1s for MIL-101-NH_2.

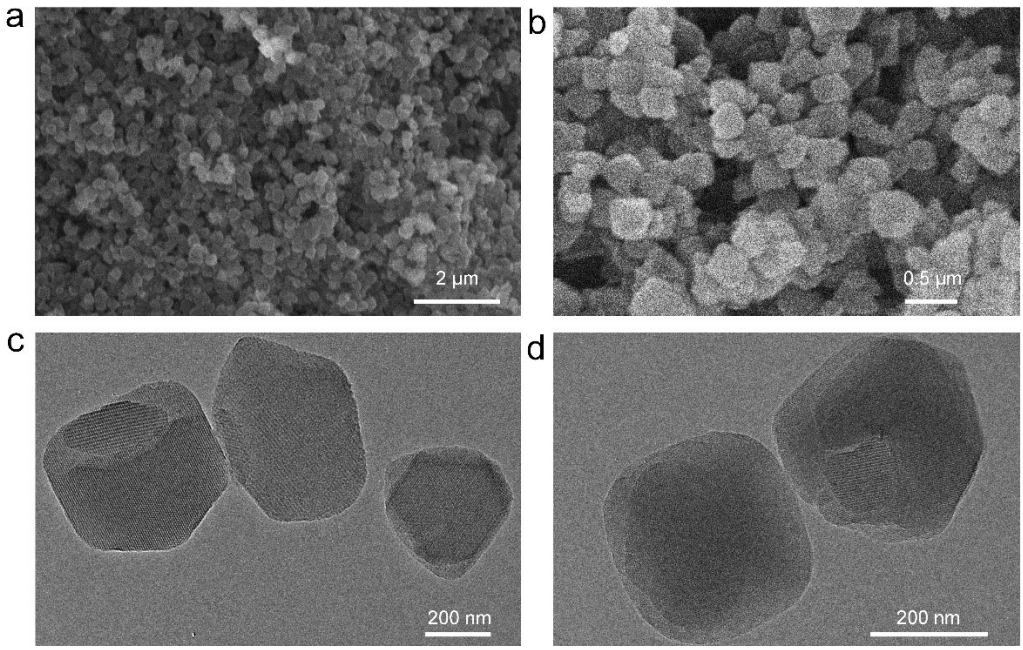

Fig. S3 SEM images of (a) MIL-101 powder and (b) MIL-101-NH_2 powder. TEM images of (c) MIL-101 powder and (d) MIL-101-NH_2 powder.

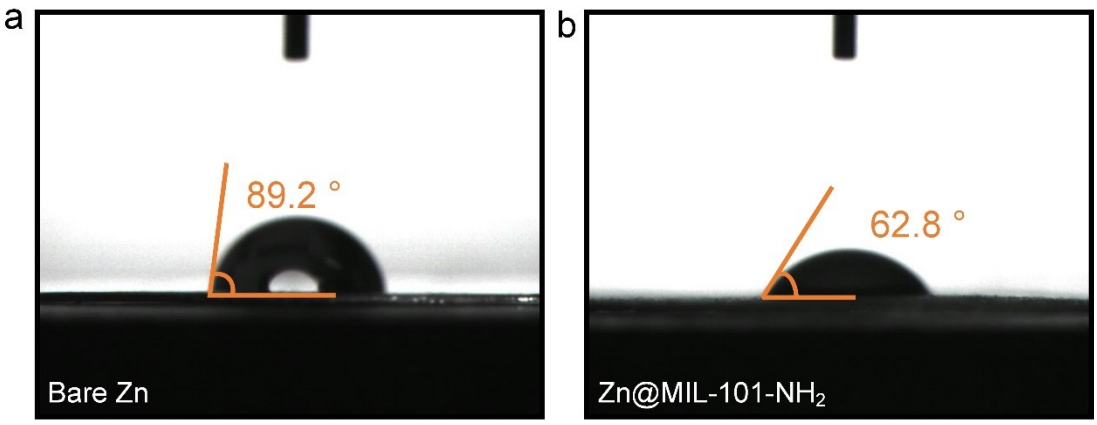

Fig. S4 Contact angle images of deionized water on the electrode surface of (a) bare Zn and (b) Zn@MIL-101-NH_2.

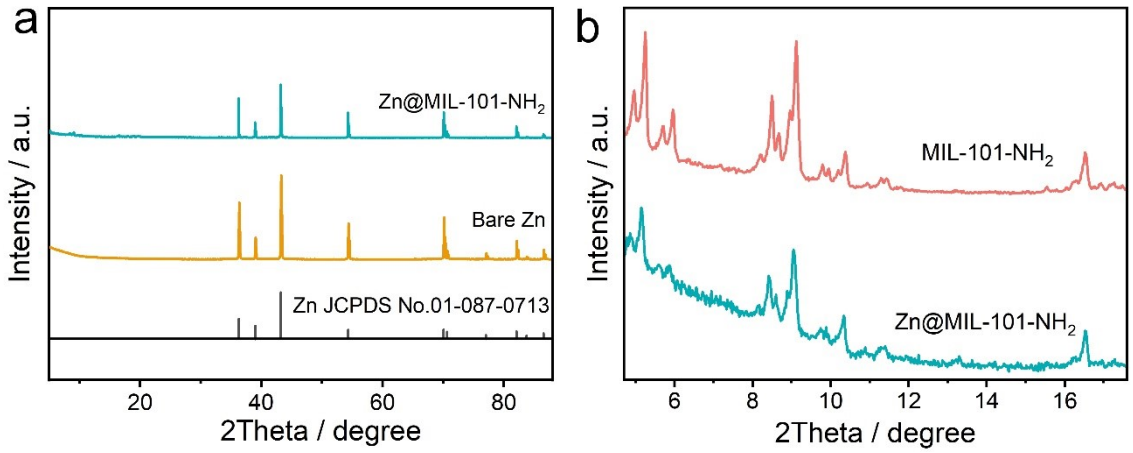

Fig. S5 XRD plots of (a) bare Zn and Zn@MIL-101-NH_2 electrodes. (b) XRD comparison of MIL-101-NH_2 powder with Zn@MIL-101-NH_2.

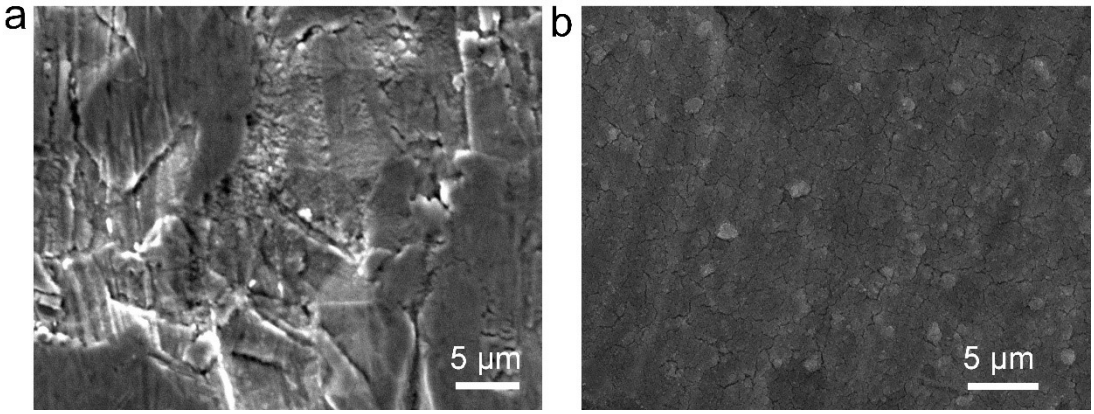

Fig. S6 SEM images of the surface of (a) bare Zn electrode and (b) Zn@MIL-101 electrode.

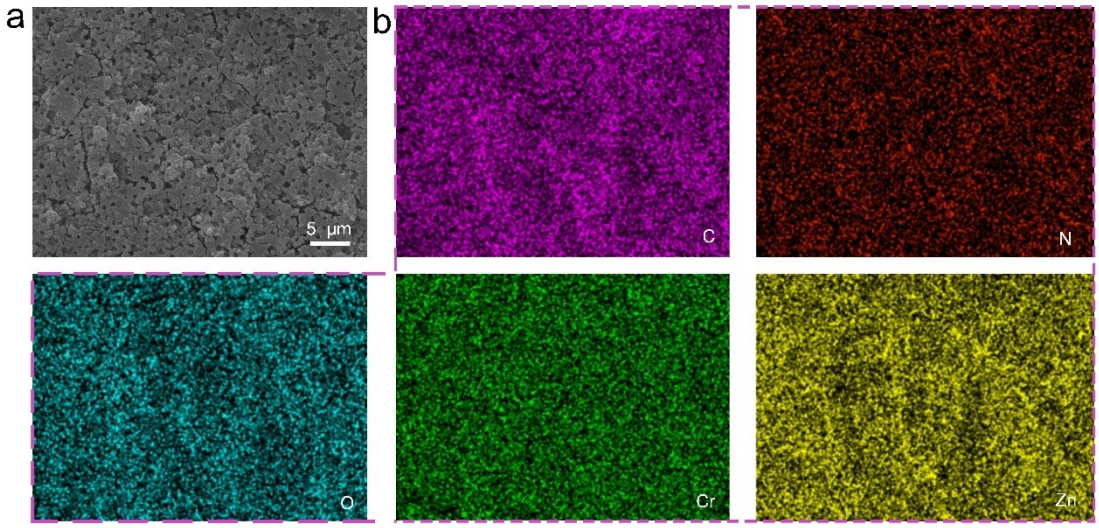

Fig. S7 SEM image of (a) Zn@MIL-101-NH_2 electrode surface and its (b) EDX image.

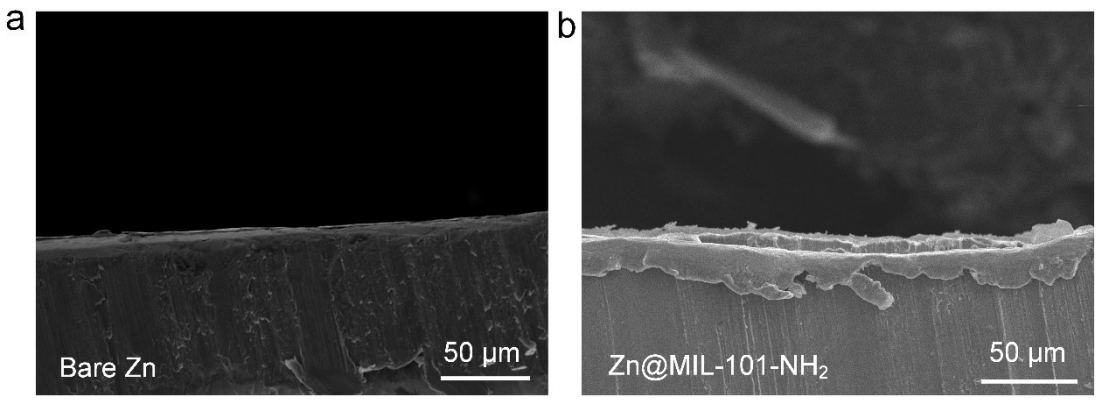

Fig. S8 (a) SEM images of bare Zn in cross-section. (b) SEM images of Zn@MIL-101-NH_2 in cross-section.

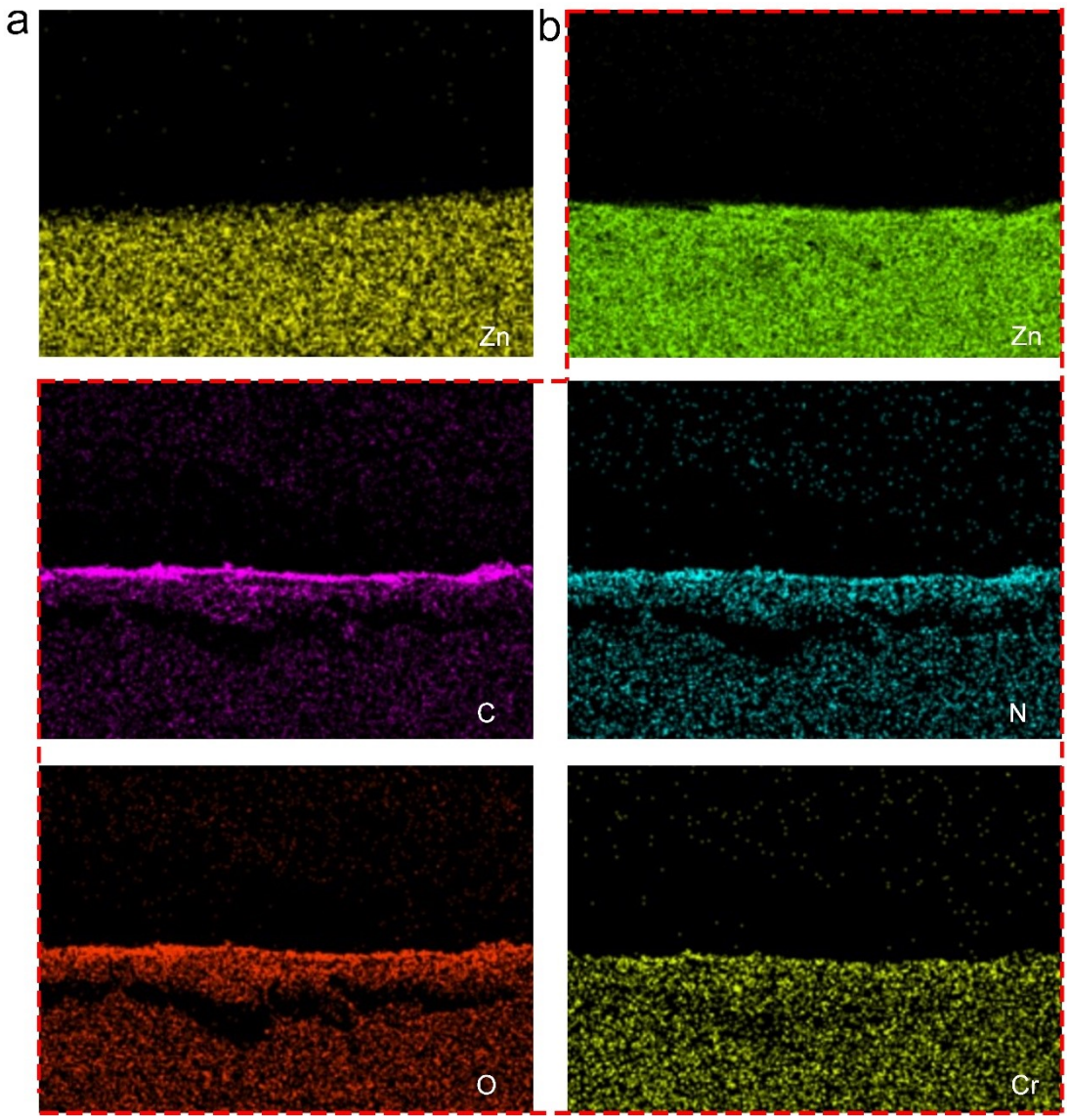

Fig. S9 (a) Element distribution of bare Zn anode cross-section. (b) Element distribution of Zn@MIL-101-NH_2 anode cross-section.

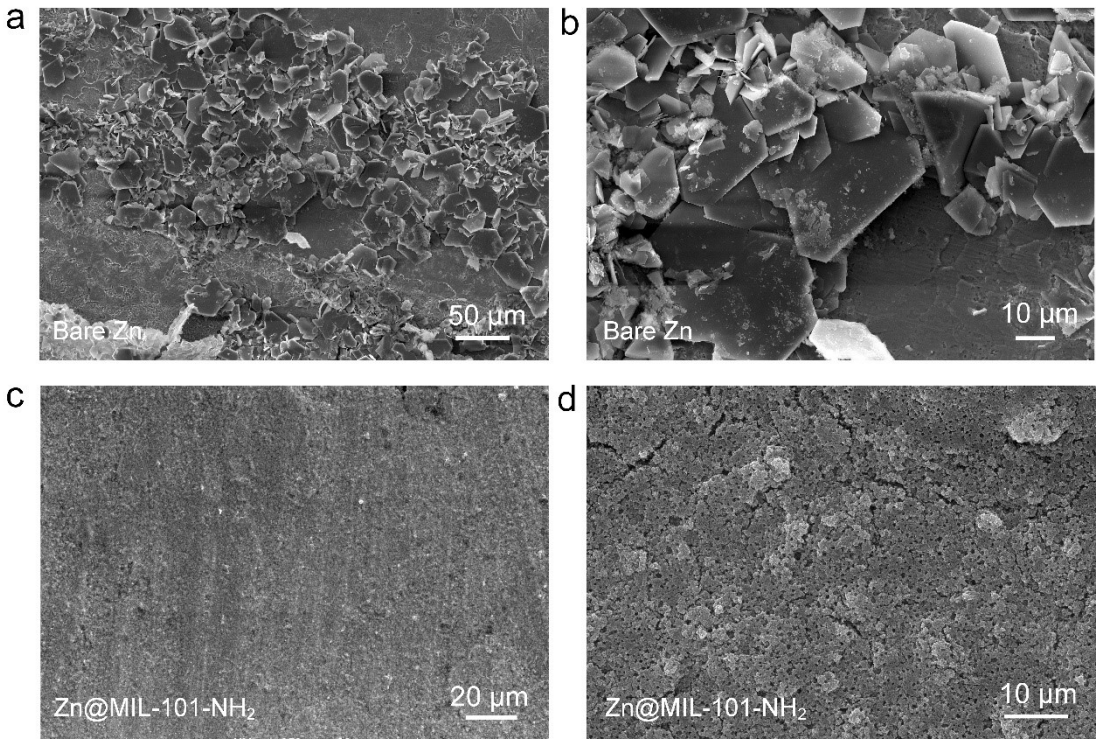

Fig. S10 SEM images of (a, b) bare Zn‖bare Zn and (c, d) Zn@MIL-101-NH_2‖Zn@MIL-101-NH_2 after three days of immersion in electrolyte solution.

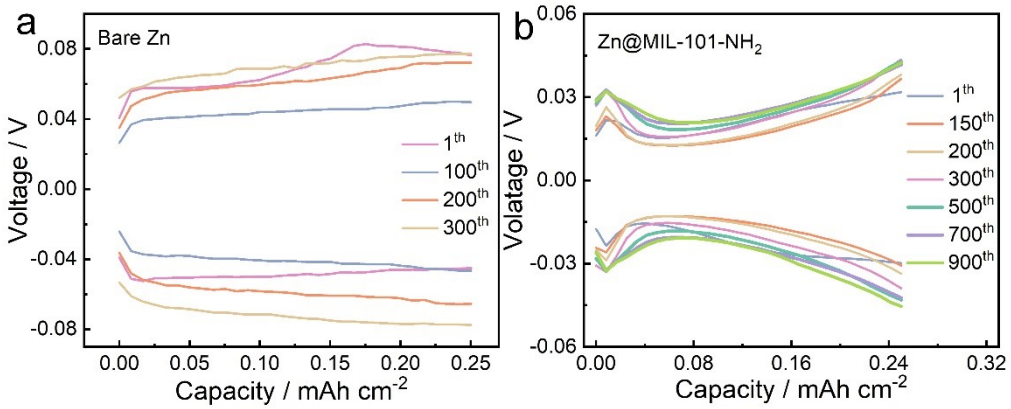

Fig. S11 Hysteresis voltage of (a) bare Zn||bare Zn, (b) Zn@MIL-101-NH_2||Zn@MIL-101-NH_2 symmetrical cells at current densities of 0.5 mA cm^{-2} for 0.25 mAh cm^{-2}.

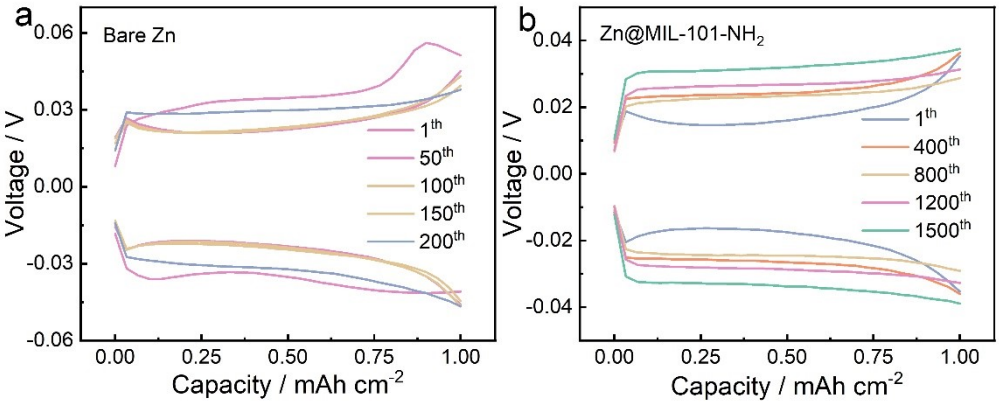

Fig. S12 Hysteresis voltage of (a) bare Zn||bare Zn, (b) Zn@MIL-101-NH_2||Zn@MIL-101-NH_2 symmetrical cells at current densities of 2.0 mA cm^{-2} for 1.0 mAh cm^{-2}.

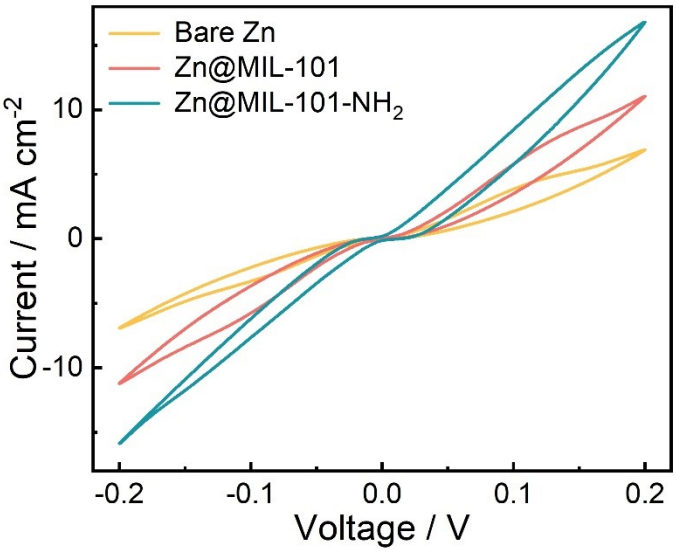

Fig. S13 Symmetric CV curves of bare Zn||bare Zn, Zn@MIL-101||Zn@MIL-101 and Zn@MIL-101-NH_2||Zn@MIL-101-NH_2.

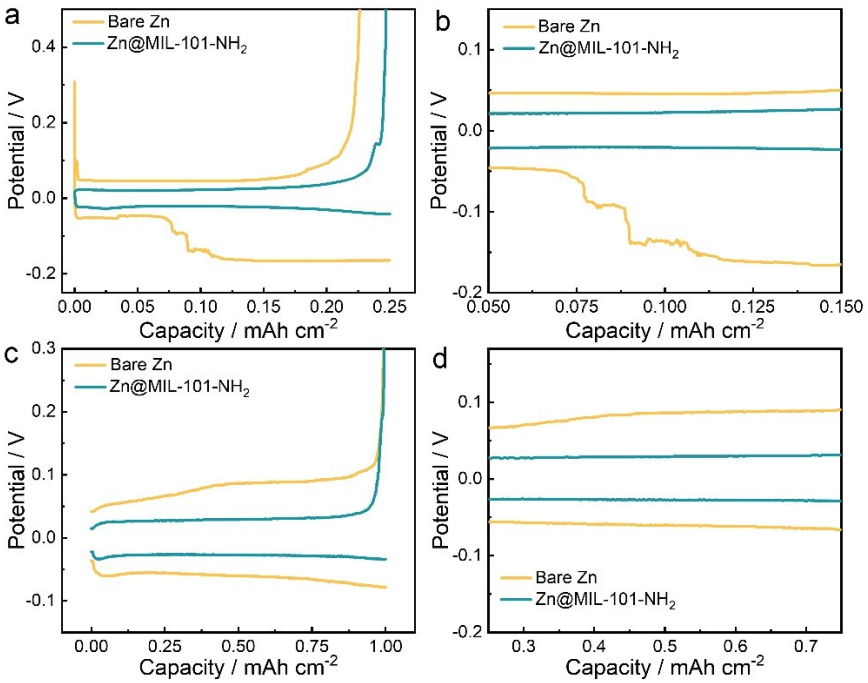

Fig. S14 (a, b) Plating stripping curves corresponding to the CE diagrams of bare Zn||Cu and Zn@MIL-101-NH_2||Cu cells with a current density of 0.5 mA cm^{-2} and a capacity of 0.25 mAh cm^{-2}. (c, d) Plating stripping curves corresponding to the CE diagrams of bare Zn||Cu and Zn@MIL-101-NH_2||Cu cells with a current density of 2.0 mA cm^{-2} and a capacity of 1.0 mAh cm^{-2}.

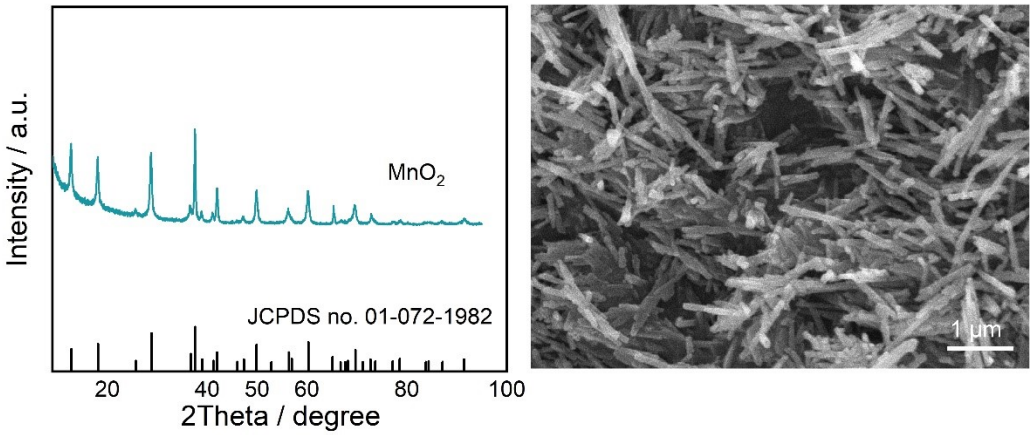

Fig. S15 (a) XRD pattern of MnO_2 cathode material. (b) The SEM image of MnO_2 cathode material.

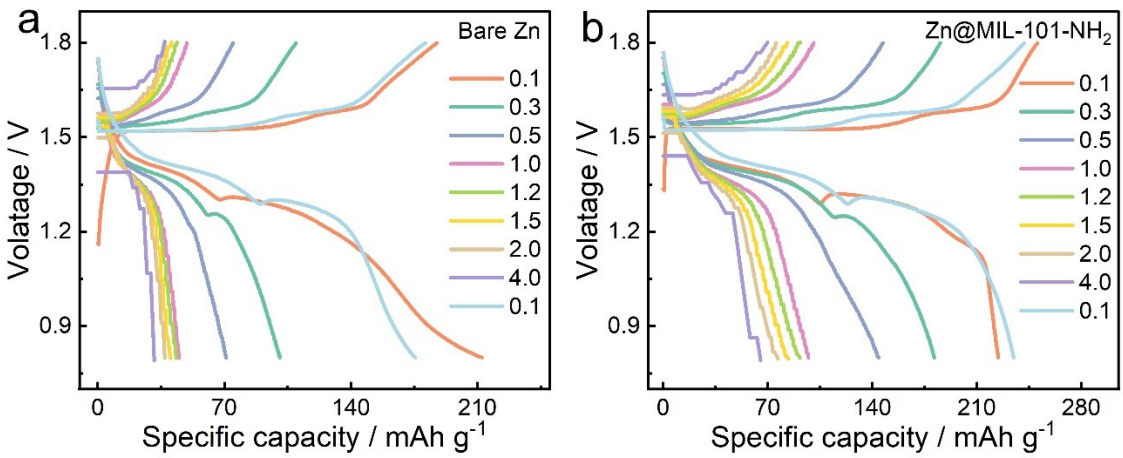

Fig. S16 Charge-discharge profiles of (a) bare Zn||MnO_2, (b) Zn@MIL-101-NH_2||MnO_2 full cells.

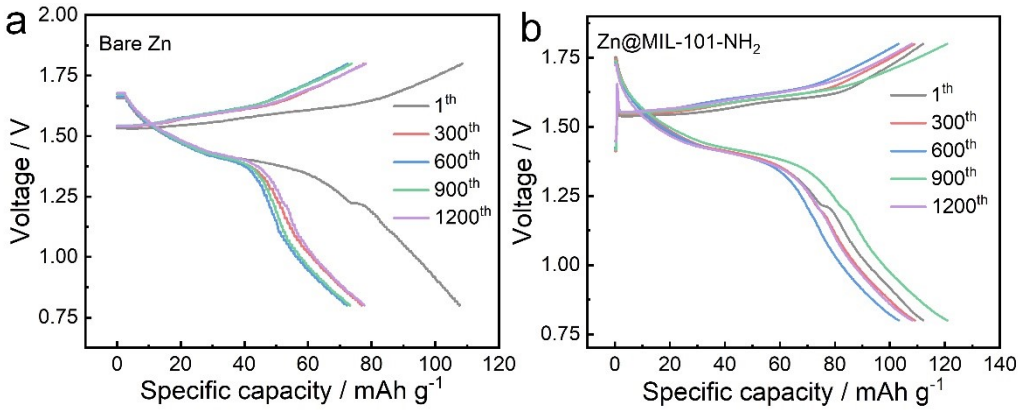

Fig. S17 Charge-discharge profiles of (a) bare Zn||MnO_2, (b) Zn@MIL-101-NH_2||MnO_2 full cells at 1.0 A g^{-1}.

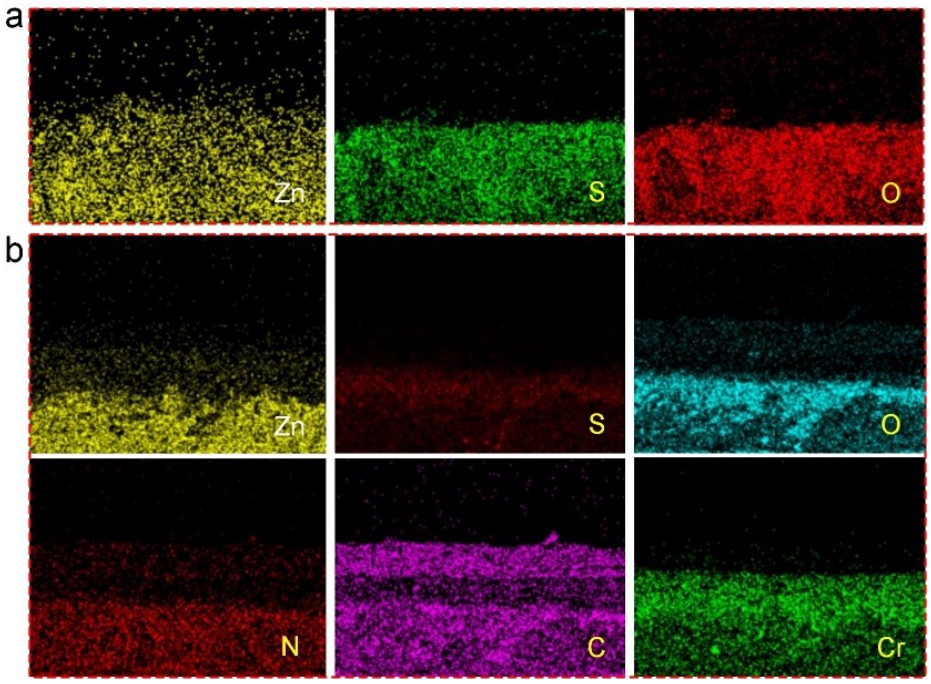

Fig. S18 (a) Elemental distribution of the cross section after bare Zn cycling. (b) Elemental distribution of Zn@MIL-101-NH_2 cross section after cycling.